Appl. Phys. B 81, 1097–1100 (2005)
DOI: 10.1007/s00340-005-1975-2

Applied Physics B
Lasers and Optics

J.S. WANG[1,✉]
G. LIN[2]
R.S. HSIAO[2,3]
C.S. YANG[3]
C.M. LAI[2]
C.Y. LIANG[2]
H.Y. LIU[2]
T.T. CHEN[4]
Y.F. CHEN[4]
J.Y. CHI[2]
J.F. CHEN[3]

Continuous-wave high-power (320 mW) single mode operation of electronic vertically coupled InAs/GaAs quantum dot narrow-ridge-waveguide lasers

[1] Department of Physics, Chung Yuan Christian University, Chung-Li 32023, Taiwan
[2] Industrial Technology Research Institute, Hsinchu 310, Taiwan
[3] Department of Electrophysics, National Chiao Tung University, Hsinchu 300, Taiwan
[4] Department of Physics, National Taiwan University, Taipei 106, Taiwan

Received: 16 February 2005/Revised version: 1 August 2005
Published online: 25 October 2005 • **© Springer-Verlag 2005**

ABSTRACT High-power 3 μm-wide narrow-ridge-waveguide lasers with ten stacks of electronic vertically coupled InAs/GaAs quantum dots in the active region were demonstrated. Unlike that from conventional uncoupled InAs quantum dot lasers, a narrow lasing spectrum was observed because the carriers tunneled in the vertical direction. Continuous-wave operation in single lateral mode yielded a kink-free output power of 320 mW with an efficiency of 0.46 W/A , and a sensitivity of lasing wavelength to temperature of 0.28 nm/K.

PACS 42.55.Px; 42.60.Jf; 78.55.Cr

1 Introduction

Quantum dots (QDs) are fascinating quantum structures because they have superior characteristics and broad applications. The application of QDs as the active region in a semiconductor laser should lead to ultra low threshold current density and extremely high thermal stability, because the density of states is described by a delta function [1]. Lasers of 1.3 μm wavelength range based on self-organized InAs QDs embedded in InGaAs quantum wells have been demonstrated to have a very low threshold current density (16 A/cm^2) [2]. The use of a ten-layer stack of long-wavelength QDs enabled the external differential quantum efficiencies to reach as high as 88% in edge emitting lasers [3] and the realization of 1.3 μm vertical cavity surface-emitting lasers (VCSELs) monolithic on GaAs substrates [4]. Another possible area of interest related to 1.3 μm emitters concerns single-mode Fabry–Perot lasers used for high-power applications. Maximov et al. [5] demonstrated 7 μm-wide ridge-waveguide single-mode QD lasers with an output power of 210 mW emitting at 1.25 μm. However, current-induced ground to excited state switching of lasing was found to limit the output power of QD lasers in the 1.3 μm region [6, 7]. Shi and Xie [8] predicted that electronic vertically coupled QD (EVCQD) lasers would exhibit a higher single-mode output power than uncoupled lasers through based on the coupled rate equations, especially when there the dot size fluctuates greatly. Moreover, the use of a thinner ECVQD active region can increase the optical model gain, increasing the optical-electrical overlap factor. Additionally, the EVCQD active region improves the carrier injection efficiency by carrier tunneling. Ustinov et al. [9] demonstrated electronic vertically coupled QD lasers with lasing wavelengths of around 1.0 μm.

This paper demonstrates high-performance single-mode highly strained ECVQD lasers with a kink-free output power as high as 320 mW under CW operation with emission wavelength of 1.22 μm.

2 Experimental

The structures were grown by solid source molecular beam epitaxy (SSMBE) in a Riber Epineat machine. Indium and gallium were supplied from conventional Knudsen effusion cells, and arsenic was supplied from a cracker source. The QDs employed herein as an active medium in the lasers, were grown in the Stranski–Krastanow growth mode by depositing InAs 2.6 monolayers (ML) at a growth rate of 0.085 ML/s and a substrate temperature of 485 °C, and then covering these layers with a 10 nm-thick GaAs layer at the same temperature; the growth temperature of the remaining layers was 600 °C. The formation of QDs was controlled in situ by monitoring the diffraction pattern of high-energy electrons (RHEED). The surface density of the QDs, estimated from atomic force microscopic (AFM) images, was around $5\times10^{10}\ \mathrm{cm}^{-2}$.

Figure 1 shows the design of the EVCQD lasers. The structure was grown on n^+-GaAs(100) substrates, consisting of a 0.3 μm thick n-type GaAs buffer layer, a 1.5 μm thick n-type $Al_{0.3}Ga_{0.7}As$ bottom cladding layer, a GaAs waveguide layer, a 1.5 μm thick p-type $Al_{0.3}Ga_{0.7}As$ upper cladding layer and a 0.4 μm thick p^+-doped GaAs contact layer. Ten stacks of InAs QDs, which were formed as described above, were symmetrically arranged in the center of the waveguide region, separated only by 17 nm thick GaAs spacer layers. Figure 1 presents a cross-sectional transmission electron microscopic (TEM) image that reveals very good vertical alignment without any dislocation. The lateral and vertical dimensions of the strain field of the QD islands are approximately 22 and 6.7 nm, respectively. (This means the vertical spacer

✉ Fax: 886-3-265-3299, E-mail: jswang@cycu.edu.tw

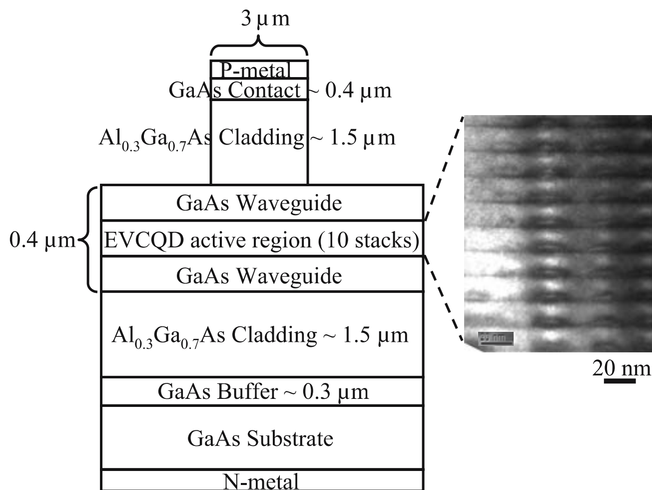

FIGURE 1 Schematic diagram of QD laser structure with narrow ridge waveguide, and the cross-sectional TEM image of ECVQD active region

thickness between QDs was around 10 nm.) The total thickness of the waveguide was 0.4 µm. The n-type and p-type cladding layers were heavily doped with Si and Be, respectively, to $1 \times 10^{18}\,\mathrm{cm}^{-3}$. Following epitaxial growth, 3 µm-wide stripes were formed using the double-channel ridge-waveguide self-aligned process with reactive ion etching. The characteristics of the laser with as-cleaved facets were measured in pulsed (1 µs, 100 kHz) and continuous wave (CW) operation.

3 Results and discussion

Figure 2 displays the room temperature photoluminescence (PL) spectrum obtained at high excitation power density (3.5 kW/cm^2), for the laser structure with etched off contact and heavily doped cladding layers. The spectrum can be fitted very well using three Gaussian peaks fitting (shown as dashed lines). The difference between the transition energy of the ground state ($E1$) and that of the excited state ($E2$) is only 32 meV. This value is half that obtained in the uncoupled case, which is approximately 70–95 meV in the 1.22–1.26 µm region [10–12]. The PL spectrum exhibit a strong overlap between ground state emission and excited state emission, because of inhomogeneous broadening due to a fluctuation in the QD size and formation of a mini-band, which is caused by the vertical coupling of the electronic wave function. The peak $E3$ may originates from the differently sized QD group because the difference between the energies $E2$ and $E3$ should be little less than that between $E1$ and $E2$, if the peak $E3$ originates from the second excited transition.

It has been shown that the electronic states can acquire a wire-like character due to vertical dot–dot coupling. This behavior can be easily examined by optical anisotropy [13–15]. Figure 3 shows the degree of linear polarization of edge-emitted PL spectra of a single-layer QDs (a) and the EVCQD laser (b). The polarization degree is defined as $P = (I_{\parallel} - I_{\perp})/(I_{\parallel} + I_{\perp})$, where $I_{\parallel}$ ($I_{\perp}$) is the PL intensity polarized in (normal to) the surface plane. For a semiconductor QD, it is well known that the optical transition is polarized along the elongated dot direction. As shown in Fig. 3a, the polarization of single-layer dots sample is perpendicular to the growth direction (transverse electric, TE, polarization dominant) with

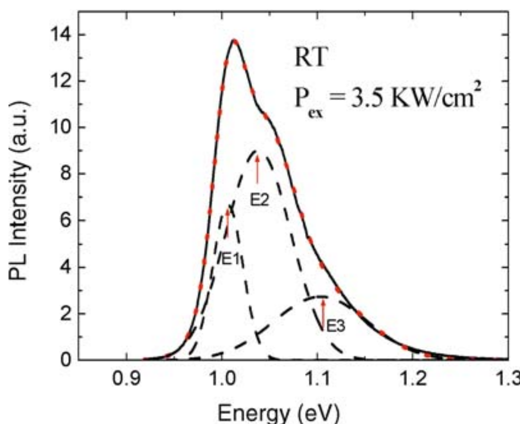

FIGURE 2 Room-temperature PL spectrum at high excitation power density, for the laser structure with etched off contact and heavily doped cladding layers. The *solid line* represents experimental data; the *three dashed lines* represent three Gaussian fitted peaks, and the *dotted line* represents the superposition of the three fitted Gaussian peaks

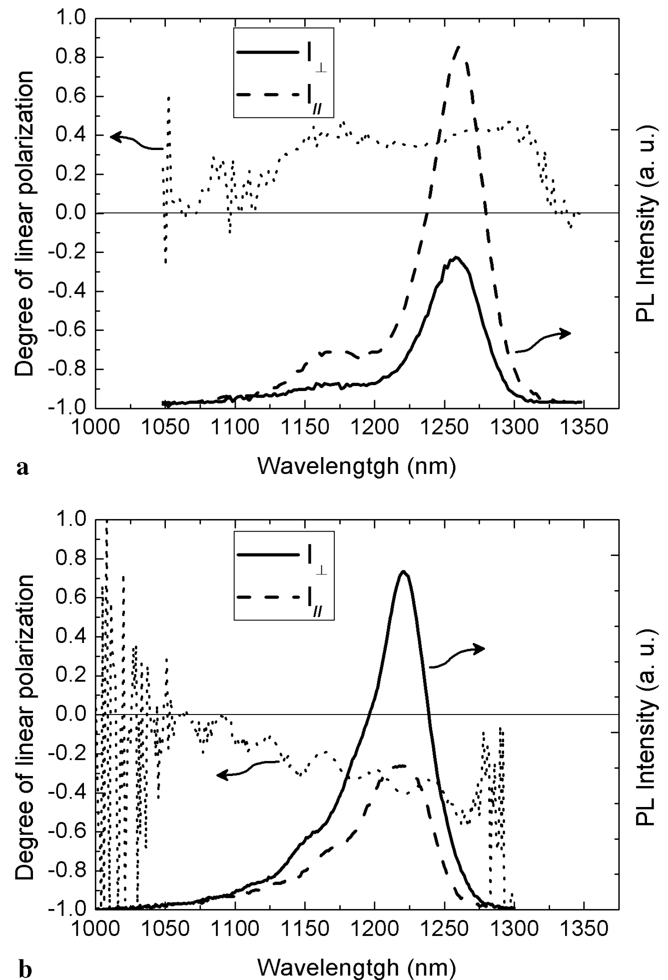

FIGURE 3 The degree of linear polarization of edge-emitted PL spectra at room-temperature. *Dashed line*: intensity spectrum of $I_{\parallel}$. *Solid line*: intensity spectrum of $I_{\perp}$. *Dot line*: polarization anisotropy spectrum. (**a**) a single-layer QDs, (**b**) the EVCQD laser

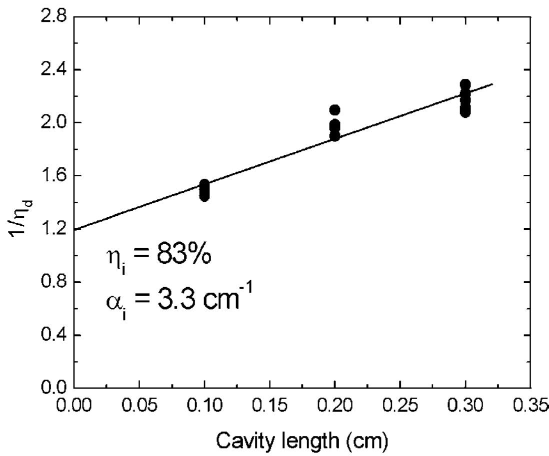

FIGURE 4 Reciprocal external quantum efficiency as a function of cavity length for 3 μm-wide ridge-waveguide lasers under pulsed operation

$P \sim 40\%$, corresponding to the in-plane elongated dot shape. With EVCQD structures, the polarization turns into transverse magnetic (TM) dominant, i.e., it is along the growth direction with a negative P value. As shown in Fig. 3b, in our case the degree of polarization is $P \sim -40\%$. It therefore provides direct evidence to confirm the vertically electronic coupling, and electronic states are strongly elongated along the growth direction.

Figure 4 displays the dependence of the reciprocal external quantum efficiency on the cavity length for 3 μm-wide ridge-waveguide lasers under pulsed operation. The internal quantum efficiency was as high as 83%, indicating good crystal quality, although as many as ten layers were used in the highly strained EVCQD active region. A maximum measured differential efficiency of 69% was obtained for a stripe-length of $L = 1$ mm. The internal loss derived from the slope of the fit curve was 3.3 cm^{-1}.

Figure 5 displays the lasing spectra of 3 μm-wide, 2 mm-long devices at an injection current of 1 A under CW operation. For comparison, a similar 1.3 μm QD laser with a conventional uncoupled InAs QD active region is also represented as a dashed line. The spectral bandwidth of the EVCQD lasers is almost half of that in the uncoupled case in which the carriers occupy the excited states at high injection current. That such a narrow lasing spectrum differs markedly from that obtained in the uncoupled case probably follows from the fact that the carriers tunnel in the vertical direction within the EVCQD active region. The results indicate that the EVCQD active region has great potential for single mode laser applications.

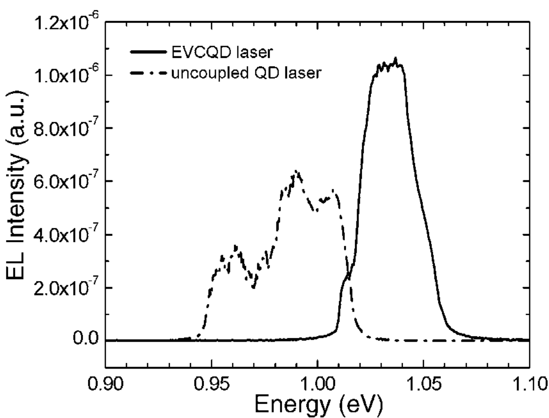

FIGURE 5 Lasing spectra of 2 mm-long cavity devices at an injection current of 1 A under CW operation. The dashed line shows a lasing spectrum for a similar 1.3 μm QD laser with a conventional uncoupled QD active region

Figure 6a shows the CW light output–current (L–I) curves at room temperature with various cavity lengths. The maximal output power measured from the device with a 3 mm-long cavity was 320 mW, with slope efficiency of 0.46 W/A, limited by thermal rollover, which occurs near the current density of 10 KA/cm^2. The insert presents the lasing spectra. Lasing occurs through only the ground state ($\sim$ 1.22 μm) with no light from excited state, even at a current density as high as 10 KA/cm^2. The lateral far-field patterns with various injection currents under CW operation, as depicted in Fig. 6b, prove single lateral mode operation up to the highest recorded power. To the best of our knowledge, this is the highest value reported for single mode QD lasers based on such 3 μm-wide narrow-ridge-waveguide devices.

Figure 7 plots the temperature-dependence of the threshold current and the lasing wavelength (at the threshold) for 3 mm-long devices under CW operation. The characteris-

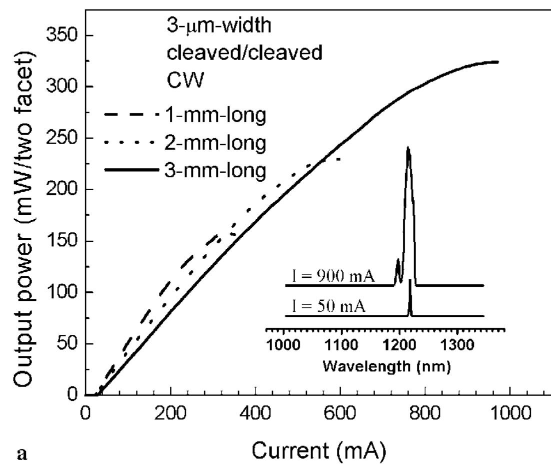

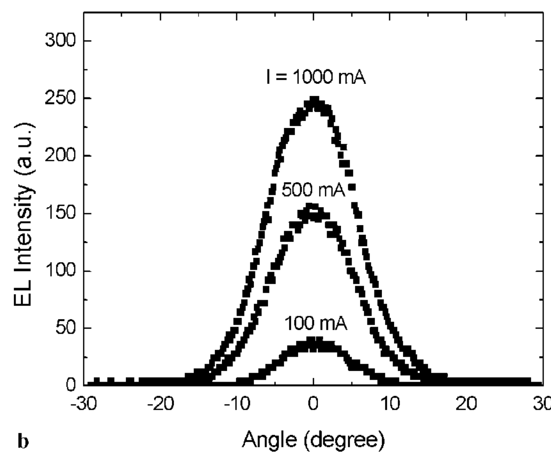

FIGURE 6 (**a**) CW light output–current (L–I) curves at room temperature for various cavity lengths. The *insert* shows the lasing spectra for the 3 mm-long cavity devices. (**b**) Lateral far-field pattern for the 3 mm-long cavity devices with various injection currents under CW operation

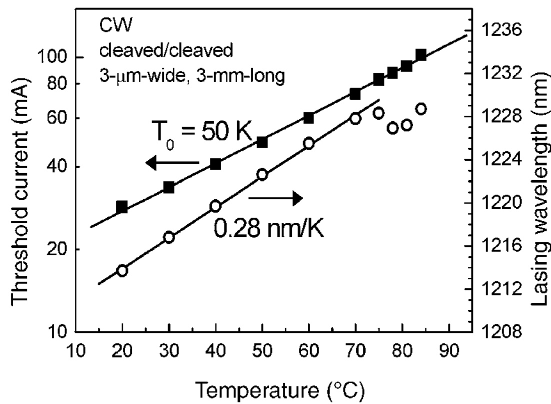

FIGURE 7 Temperature-dependence of the threshold current and lasing wavelength (at threshold) for the 3 mm-long cavity devices under CW operation

tic temperature (T_0) in the range 20–85 °C is 50 K. According to the low confinement design (GaAs waveguide and $Al_{0.3}Ga_{0.7}As$ cladding layers), this T_0 is in the normal range [16], and can be improved by optimizing the structural design in the future [3, 17]. The lasing wavelength is 1.223 μm at room temperature, and slowly shifts toward longer wavelengths, with a coefficient of 0.28 nm/K, which is much less than that in the uncoupled case, which is around 0.45 nm/K [3]. However, the shift in lasing wavelength becomes saturated when the temperature exceeds 75 °C because the carriers occupy higher energy states at higher temperature, compensating for the decrease in the energy band-gap as the temperature increases.

4 Conclusion

High-quality narrow-ridge-waveguide electronic vertically coupled InAs/GaAs QD lasers with an emission wavelength of 1.22 μm were demonstrated. The internal quantum efficiency of 83% and external differential quantum efficiency of 69% were obtained for 1 mm-long devices, indicating good crystal quality, although an as many as ten layers were involved in the high-strain EVCQD active region. Unlike in conventional uncoupled InAs quantum dot lasers, a narrow lasing spectrum was observed because carriers tunneled vertically. A record room-temperature CW single lateral mode output power of 320 mW was obtained.

ACKNOWLEDGEMENTS The authors would like to thank the national science council of the Republic of China, Taiwan, for financially supporting this research under Contract No. NSC 94-2112-M-033-005. K.Y. Hsieh is appreciated for making TEM measurements, as well as A.R. Kovsh, A.E. Zhukov and D.A. Livshits for their valuable discussions.

REFERENCES

1 Y. Arakawa, H. Sakaki, Appl. Phys. Lett. **40**, 939 (1982)
2 G.T. Liu, A. Stinz, H. Li, T.C. Newell, A.L. Gray, P.M. Varangis, K.J. Malloy, L.F. Lester, IEEE J. Quantum Electron. **36**, 1272 (2000)
3 A.R. Kovsh, N.A. Maleev, A.E. Zhukov, S.S. Mikhrin, A. P. Vasil'ev, Y.M. Shernyakov, M.V. Maximov, D.A. Livshits, V.M. Ustinov, Z.I. Alferov, N.N. Ledentsov, D. Bimberg, Electron. Lett. **38**, 1104 (2002)
4 J.A. Lott, N.N. Ledentsov, A.R. Kovsh, V.M. Ustinov, D. Bimberg, 16th Annual Meeting IEEE LEOS **2**, 499 (2003)
5 M.V. Maximov, L.V. Asryan, Y.M. Shernyakov, A.F. Tsatsul'nikov, I.N. Kaiander, V.V. Nikolaev, A.R. Kovsh, S.S. Mikhrin, V.M. Ustinov, A.E. Zhukov, Z.I. Alferov, N.N. Ledenstov, D. Bimberg, IEEE J. Quantum Electron. **37**, 676 (2001)
6 A.E. Zhukov, A.R. Kovsh, D.A. Livshits, V.M. Ustinov, Z.I. Alferov, Semicond. Sci. Technol. **18**, 774 (2003)
7 A. Markus, J.X. Chen, C. Paranthoën, A. Fiore, C. Platz, O. Gauthier-Lafaye, Appl. Phys. Lett. **82**, 1818 (2003)
8 B. Shi, Y.H. Xie, Appl. Phys. Lett. **82**, 4788 (2003)
9 V.M. Ustinov, A.Y. Egorov, A.R. Kovsh, A.E. Zhukov, M.V. Maximov, A.F. Tsatsul'nikov, N.Y. Gordeev, S.V. Zaitsev, Y.M. Shernyakov, N.A. Bert, P.S. Kop'ev, Z.I. Alferov, N.N. Ledensov, J. Böhrer, D. Bimberg, A.O. Kosogov, P. Werner, U. Gösele, J. Cryst. Growth **175/176**, 689 (1997)
10 H. Saito, K. Nishi, Y. Sugimoto, S. Sugou, Electron. Lett. **35**, 1561 (1999)
11 K. Mukai, Y. Nakata, K. Otsubo, M. Sugawara, N. Yokoyama, H. Ishikawa, Appl. Phys. Lett. **76**, 3349 (2000)
12 H. Chen, Z. Zou, O.B. Shchekin, D.G. Deppe, Electron. Lett. **36**, 1703 (2000)
13 P. Yu, W. Langbein, K. Leosson, J.M. Hvam, N.N. Ledentsov, D. Bimberg, V.M. Ustinov, A.Y. Egorov, A.E. Zhukov, A.F. Tsatsul'nikov, Y.G. Musikhin, Phys. Rev. B **60**, 16 680 (1999)
14 I.L. Kerstnikov, N.N. Ledentsov, A. Hoffmann, D. Bimberg, Phys. Status Solidi A **183**, 207 (2001)
15 Z. Xu, D. Birkedal, J.M. Hvam, Z. Zhao, Y. Liu, K. Yang, A. Kanjilal, J. Sadowski, Appl. Phys. Lett. **82**, 3859 (2003)
16 L.F. Lester, A. Stintz, H. Li, T.C. Newell, E.A. Pease, B.A. Fuchs, K.J. Malloy, IEEE Photonics Technol. Lett. **11**, 931 (1999)
17 O.B. Shchekin, J. Ahn, D.G. Deppe, Electron. Lett. **38**, 712 (2002)